International Journal of Science and Research (IJSR)
ISSN (Online): 2319-7064
Index Copernicus Value (2016): 79.57 | Impact Factor (2015): 6.391

Numerical Simulation of a Building Collapse on Sandy Clay of Douala City in Cameroon

A. Abanda[1], Dr. D. Fokwa[2], P. Eba'a[3]

[1]Assist. Prof, Department of Civil Engineering, Laboratory of Mechanic, University of Douala, Cameroon

[2]Professor and Head of the Civil Engineering Department, Laboratory of Mechanic, University of Douala, Cameroon

[3]Student PhD, Civil Engineering Department, Laboratory of Mechanic, University of Douala, Cameroon

Abstract: ***Since land-use losses are very costly for the community, it is important to consider appropriate construction solutions. In the particular case of the city of Douala, we want to understand the mechanisms of triggering a progressive collapse of infrastructural origin. A global numerical approach has been used. It was based on hypotheses concerning the modification of the initial framework by taking off a vertical carrier, the imposition of a displacement and the observation of the deformations as a function of time. The numerical simulation from the Cast3M code allowed to analyze the behavior of the soil-structure interface and its influence on the superstructure. As a result, the high compressive forces at the point of application of the displacement cause a failure due to the settlement of the soil within the zone influenced by the stress bubble, hence the need to adapt the geometry of foundations to geotechnical context. The study revealed a breaking stress of 0.1Mpa. The deformation diagrams show that ruin occurs following a localized rupture of the soil, the appearance and then the propagation of cracks on the framework, before the collapse by domino effect of the whole.***

Keywords: Soil-structure, interaction, stress, displacement, collapse

1. Introduction

For many decades design rules have for structures have been proposed, in an attempt to prevent the instability or collapse of civil engineering works. Despite the progressive refinement of these rules over the years and in particular the different developments of the BA 45, BAEL 83 rules up to the current Eurocodes relating to reinforced concrete constructions, the analytical approaches have shown their limit in taking into account certain phenomena (Nour El Houda Khitas, 2017, Medjahed Amina, 2012) [1, 2]. It is difficult for these rules based on a statistical analysis of the collapse process to predict the behavior resulting from the soil-structure interaction (Allen, T., 2009) [3]. Faced with this complexity, the present study, which aims at predicting the behavior of geotechnical structures in order to propose constructive provisions relevant to their stability, is based on a numerical simulation of a G+4 building using the code of Cast3M. This tool allows not only to understand the overall behavior of the structure, to solve nonlinear problems, but also to obtain results with a cost and a non-prohibitive time (Kaewkulchai et al., 2004) [4]. Given the vulnerability of constructions erected in compressible soils in general, a predictive study of the behavior of the substratum, seat of the localization of the deformations and concentration of the significant stresses proves necessary for a good infrastructural conception (Sébastien Burton and al. 2017) [5]. The purpose of this article is to analyze the interface structure and clay-sandy soil of the city of Douala, in order to achieve a better understanding of the process of the gradual collapse of a building under pressure compression.

2. Methodology

2.1 Principle of use of the software

Cast3M is a calculation software used for solving problems of thermal, chemical or mechanical order. Serves more generally for solving partial differential equations by the finite element method. This calculation code was developed in the Department of Mechanics and Technology (DMT) of the Commissariat à l'Energie Atomique (CEA) (E. Le Fichoux, 2011) [6]. It has several advantages including flexibility and ease of adaptation of the user. its procedural organigram is as follows:

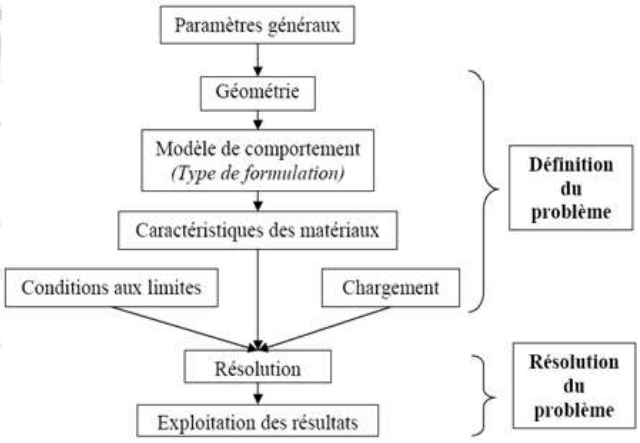

Figure 1: Calculation Model

2.2. Problem solving procedure

2.2.1. Physical Models: This is the geometric presentation of the building's skeleton whose infrastructure is studied. It is adapted to the physical and numerical modeling of soil-structure interactions, considered in the 2D portal, (Xiang Wei Zhang, 2011) [7]. The infrastructure of this study has been analyzed under two main assumptions:

- The clay soil in the defined area is deformable under load and bounded in length at 5.00m on either side of the end posts of the gantry, for a depth of 4.90m.
- The elements of reinforced concrete frame are of respective sections (20 x 30) for the poles and (1.50 x

1.50) for the soles. The total height of the framework is 17.00m.

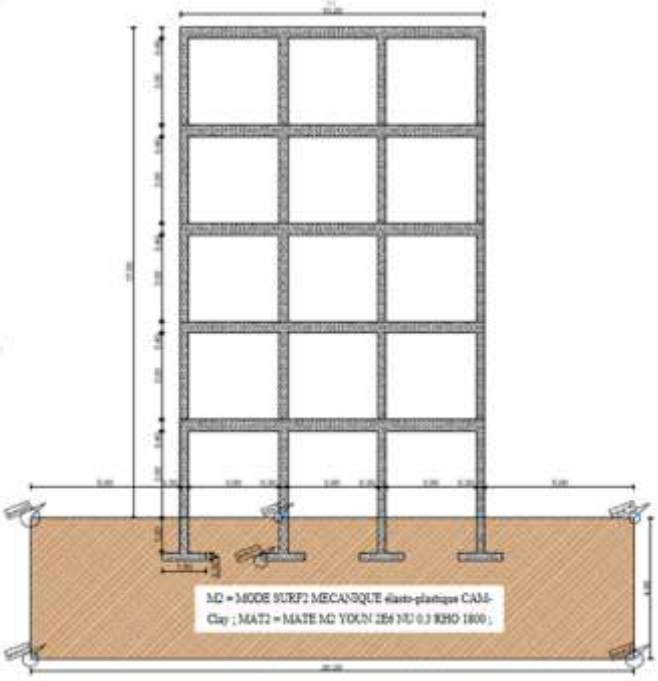

Figure 2: Infrastructure Soil Modeling

The characteristics (density, Young's modulus, Poison coefficient) taken into account in Figure 2 above are those of the sandy-clay soil of the city of Douala [8].

2.2.2. Meshing

We have geometrically discretized the domain of analysis, so that we can later associate a formulation in finite elements to the geometric support. This process inspired by several authors (P. Fajfar.P, et al. 2005) [9] allows to create objects in meshed form (points, lines, surfaces) using geometric operators. For the realization of this mesh, the method used in this article is the following:

- *The construction of the points:* we identified all the coordinates of the points of our physical model then we introduced the data by executing the procedure of the mesh as explained above.
- *The construction of lines*: For the outer contour, the direction of construction of the lines is the opposite direction of the needles of a watch and for the inner contour we used the clockwise direction to let appear the elements carrying of the structural. The resulting mesh of this process is shown in Figure 2 below.

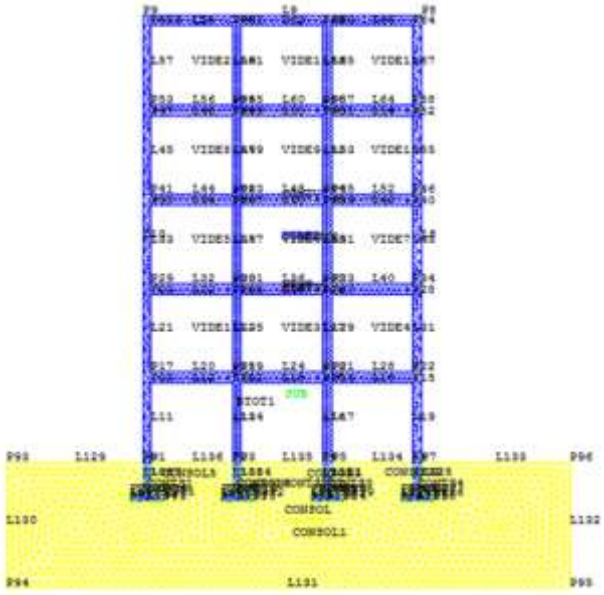

Figure 3: Infrastructure and superstructure mesh

2.2.3 Choice of model of material behaviors

Because it permits us to treat the problem of soil-structure interaction at one whole point, (O.C. Zienkiewiez et al. 2005, Badel B.P, 2001) [10, 11], we have chosen the global model (or direct method). This numerical model offers the possibility of analyzing the complete system in a single step, and the overall model also includes any non-linear behavior of soil and structure and any heterogeneity present in the soil. This type of method can be addressed by the contact conditions at the soil-structure interface and the radiation and energy dissipation condition in the infinite part of the unbounded soil (AA Becker, 1992) [12]. Technic used to deal with this condition has been the used of absorbent boundaries, finite element-boundary element coupling and finite element- infinite elements coupling. It facilitates the construction of the matrices constituting the algebraic system of differential equations which describe the dynamic motion of the structure. Under this hypothesis, the vectoral writing of the tensors of the constraints of the two-dimensional deformations, according to the elastoplastic model of CAM-Clay to generate the stresses and the deformations of the soil is expressed by the following equations:

$$\varepsilon_{ij} = \frac{(1+\nu)}{E}\sigma_{ij} - \frac{\nu}{E}\sigma_{kk}\delta_{ij}\ ;$$

$$\sigma_{ij} = \frac{(1+\nu)}{E}\varepsilon_{ij} - \frac{E\nu}{(1+\nu)(1-2\nu)}\sigma_{kk}\delta_{ij} \quad (1)$$

The stability of the material (reinforced concrete) imposes the following conditions on the parameters E and ν:

$E > 0$ *and* $-1 \leq \nu \leq 0,5$

Où: **E**= Young's modulus; ν = Poisson Coefficient ; δ_{ij} = Kronecker Indice

$$\sigma = \{\sigma_{11}\ \sigma_{22}\ \sigma_{12}\ \};\quad \varepsilon = \{\varepsilon_{11}\ \varepsilon_{22}\ \varepsilon_{12}\ \} \quad (2)$$

The deformation-displacement relation is written in the following matrix form:

$$\{\varepsilon_{11}\ \varepsilon_{22}\ 2\varepsilon_{12}\} = \left[\frac{\partial}{\partial_{x1}} 0\ 0\ \frac{\partial}{\partial_{x2}}\ \frac{\partial}{\partial_{x2}}\ \frac{\partial}{\partial_{x1}}\right] \{U_1.U_2\} \quad (3)$$

Let Ɛ=Su; then the stress-displacement relationship.

Becomes:

$$\sigma=\{\sigma_{11}\ \sigma_{22}\ \sigma_{12}\}=[d_1\ d_2\ 0\ d_2\ d_1\ 0\ 0\ 0\ d_3\ ]$$
$$[\frac{\partial}{\partial_{x1}}\ 0\ 0\ \frac{\partial}{\partial_{x2}}\ \frac{\partial}{\partial_{x2}}\ \frac{\partial}{\partial_{x1}}\ ]\ \{U_1\ .\ U_2\ \};\ \ Let\ \sigma = DS_U$$
$$[\frac{\partial}{\partial_{x1}} 0\ 0\ \frac{\partial}{\partial_{x2}}\ \frac{\partial}{\partial_{x2}}\ \frac{\partial}{\partial_{x1}}]\{U_1.U_2\};Let\ \sigma = DS_U \quad (4)$$

Where $d_3=\frac{1}{2}\ (d_1-d_2)\ d_1$ et d_2 are given in the case of plane stress by

$$d_1 = \frac{E}{1-\mu 2};\quad d_2 = \mu d_1$$

and in the case of plane stress by:

$$d_1 = \frac{E(1-\mu)}{(1+\mu)(1-2\mu)};\quad d_2 = \frac{\mu d_2}{1-\mu}$$

2.2.4 Boundary conditions

Before loading, we blocked the soil boundary associated with the study. This blocking concerns at first the lines L_{131}, L_{130}, L_{132}, along Uy and along Ux, then the line L_{111} which represents the base of the sole of the column under which the displacement will be carried out for the simulation of the settlement (Figure 3). These boundary conditions allowed us to construct the stiffness matrix that will allow the program to generate calculations of the linear and nonlinear behavior of the material. For the matrices of rigidity, we have for equation:

RIGT = RIGI MODT MATOT (for taking into account the constitutive laws of the materials and the adopted model).

RIGTOT = RIGT AND CLTOT (for taking into account the total rigidity and the limiting conditions).

2.2.5 Loading Principle

For the loading, we imposed a displacement under a sole (foundation footing), as to simulate the suppression of an initially existing post, with the aim of creating a more important space (current practice of the masters of wormy works). This operation will allow us to study the behavior of the soil at different points and to analyze the disorders in the building. In addition, we present a function U (t) = U0 + Δt which will allow the analysis of the displacements of the infrastructure and its repercussions on the superstructure. This analysis is done by imposing a displacement and a time (t), in order to appreciate from the time evolution, the evolution of the value of displacement. The point of application of the loading is shown below.

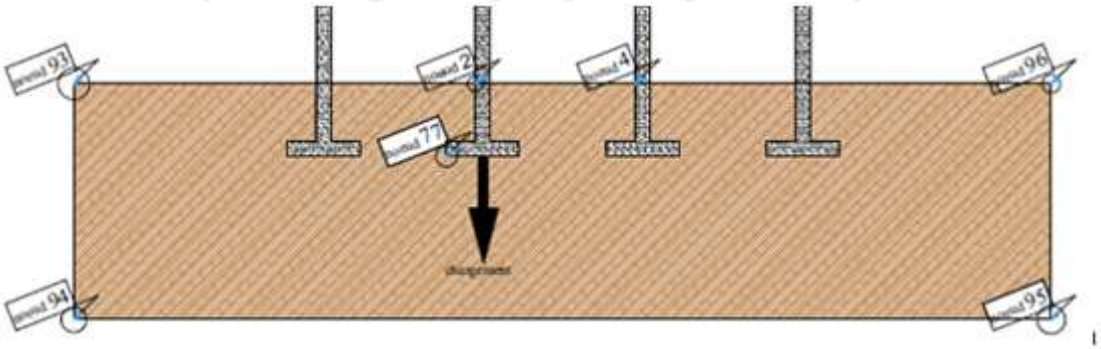

Figure 4: Loading patterns under the footing of the columns

2.2.6 Solving the problem

The resolution of our problem goes through the following operations:

We imposed a displacement (Δu) on the line (L_{111}). The value of this displacement is evolutionary within the fixed time interval. We can then better understand the progressive and global behavior of the gantry (the infrastructure and the superstructure), and generated a list (LIT1) that calculates the displacements as a function of time and can draws the line D = U (t). We used a nonlinear loading by carrying out a PASAPAS calculation and obtained a table (TAB1) to store the data and write the equations which make it possible to extract the curves of stress-displacement, the diagrams of the values of Von Mises, the deformation diagrams, damage charts and curve then start the program. The program highlights the different behavior curves that are extracted for interpretation using the @EXEL procedure.

Table 1: Material properties

Constant	Value	Note
RHO	2500 Kg.m^{-3}	Density of concrete
YOUN	2,1 10^{11} Pa	Young's Modulus
NU	0,3	Poisson Coefficient
AT	0.8E0	Mazars Concrete Coefficient
BT	1.7E+4	Coefficient of Mazars concrete in compression
BE	1.06E+0	Mazars Concrete Coefficient
AC	1.4E+3	Tensile strength
BC	1.9E+3	Compressive strength
KT	1.E+4;	Coefficient of Mazars concrete in tension

3. Results and Discussion

The overall behavior of the framework will be analyzed from the responses of certain points of the geometric model which can be identified from Figure 4 and the different stress-displacement diagrams obtained.

3.1 Infrastructure stress-displacement curves

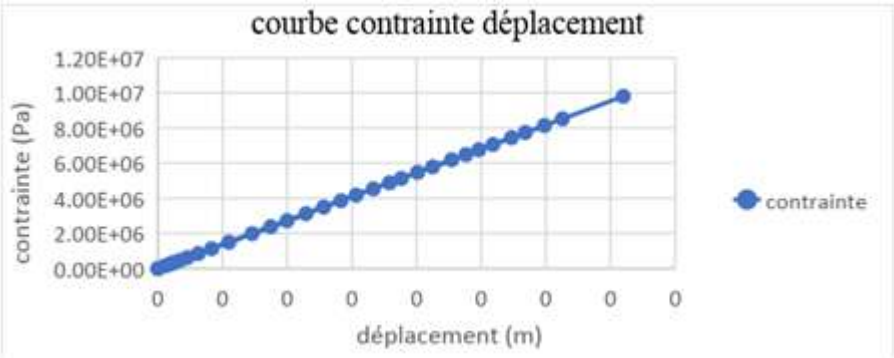

It can be observed that at point 77 located at the reinforced concrete footing interface and the ground, the elastic limit is reached for a stress value in the soil $(\sigma_{yymax})= 1{,}00Mpa$. In this situation, the soil-structure interaction exhibits monotonic behavior that obeys Hooke's law because at the beginning of the loading, the soil stress remains higher than the load. This is the case of moderate loads on a floor. This analysis confirms the results of the studies (Imen SAID, 2006, Omar Benzaria, 2012) [13, 14], which shows that the stress in the soil increases proportionally with the increase in its normal stress imposed before flow.

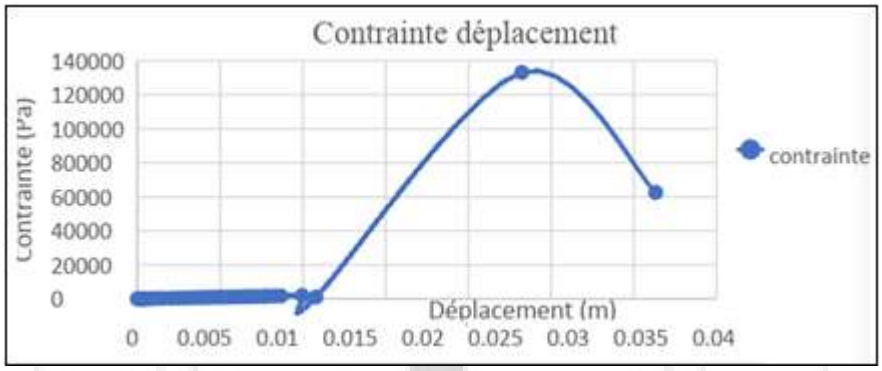

Figure 5(b) Constraint-displacement curve along YY, P2

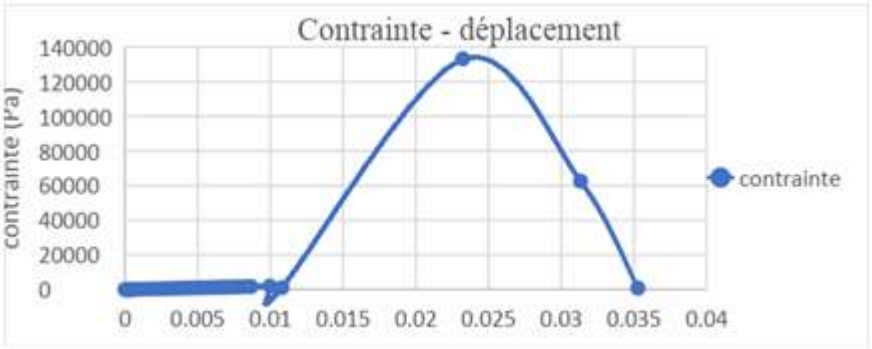

Figure 5(c): Stress-displacement curve along XX, P77

We find out that points **P2** and **P77** located on the impact zone where the soil stress is quite low as shown by the displacement value (cm). From 1 to 2.3cm, the soil has an elastic behavior whose stress rises to 1.33bars. The plastic behavior that follows, limits its effect under a displacement of 3.1 cm, synonymous with a high load that the soil stress of sandy clay type cannot resume under the section of the footing 1.50m x 1.50m. These results also prove that the nature of the soil and the density of the load are triggering elements of vulnerability of the infrastructures which can cause for the compressible soils a rupture by shearing. This analysis reinforces that of Nour El Houda Khita (2017) just as it joins the results obtained by other works (Ligil Mathew et al, 2014, Zasiah Tafheem et al, 2016) [15, 16], after the simulations collapses on swelling clay soils. The total flow occurs when under increasing deformation, the substratum reaches a stress of 0.5 bars. On the other hand, at point 77, the soil has the same behavior but records, under displacement, a plastic phase up to a stress equal to 0.00794 bar before breaking. This is due to the fact that the footing contributes to taking up the descending pressure through its section, thus avoiding a sudden rupture of the ground as observed in point 2. In fact, the liquefaction of the soil is due to the concentration of the constraints on this interface. quite thin. This behavior in compression of the soil is translated by disorders in superstructure by domino effect.

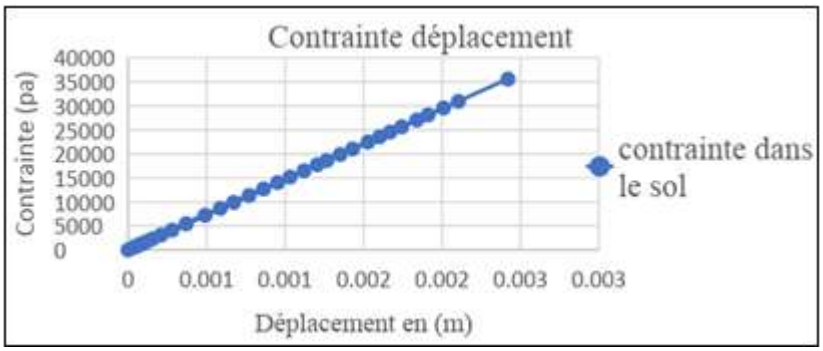

Figure 5(d): Stress-strain curve along XX, P4

At **point 4**, the soil has a monotonous linear behavior and the elastic limit is reached for a stress value of 0.35 bar for a displacement of 2.3 mm. This can be explained by the fact that the point is located on an interface at a distance of 3.00m from the point of application of the imposed displacement, an area that the stress bubble does not significantly affect (Figure 4 & Von Mises diagrams). The displacement and the normal stress vary proportionally with a constant K ratio. This analysis matches that of the "Final Report" resulting from the experimental study of mechanisms for triggering the phenomena of instability of infrastructures (M. Vincent et al., 2006) [17].

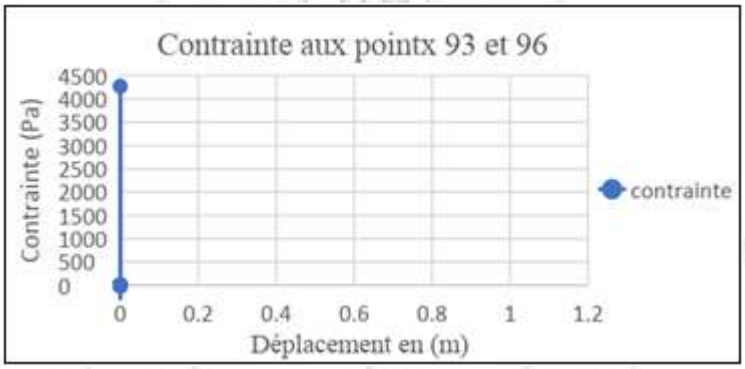

Figure 5(e) Stress-displacement curve according to XX, points 93 and 96

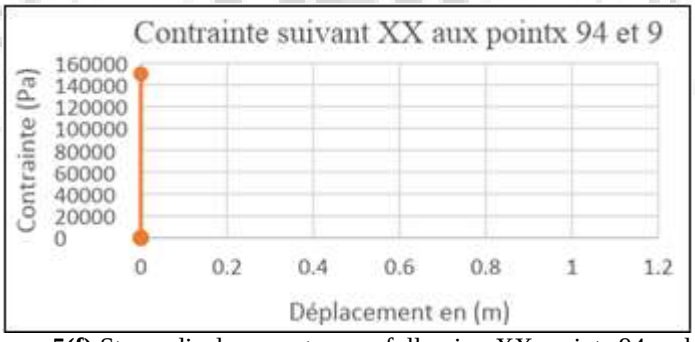

Figure 5(f) Stress-displacement curve following XX, points 94 and 95

Points 93 and 96 represent the upper boundary of our boundary. We note that despite the vertical displacement of the soil imposed under one of the intermediate flanges in the delimited area, the stress remains constant for a value of 0.04bars. On the other hand, the constraint on the lower boundary, identifiable by points 94 and 95 for a depth of study of 4.90m, is 1.5 bar, the value of the allowable stress of the ground at rest. In other words, the constraint bubble does not reach the points 94 and 95 of our mesh. The effect of settlement is not felt at a certain depth under the footing. There is therefore no compaction or breakage by shearing or punching. The finding of this simulation confirms the results highlighted by some works (Hazen, Hunter, 1969, Wolf, J., 1988) [18, 19]. They demonstrate the interest of anchoring foundations in compressible terrain.

3.2 Von Mises stress diagrams

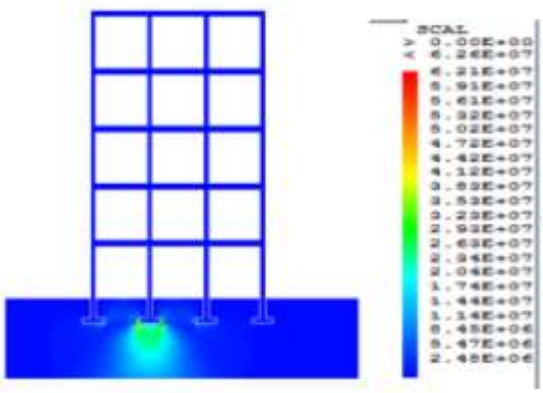

Figure 6(a): The Von Mises's diagram max. at time 30 s

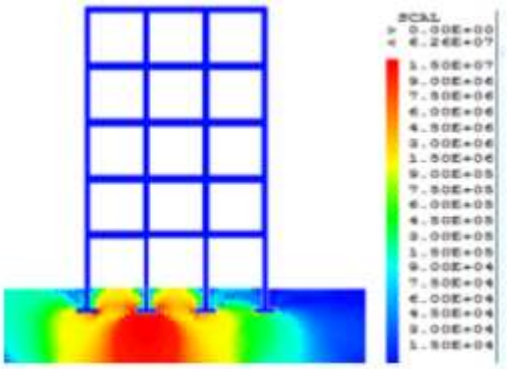

Figure 6(b): The Maximum Von Mises's diagram +liso stress values
Value of contraint at time 30 s

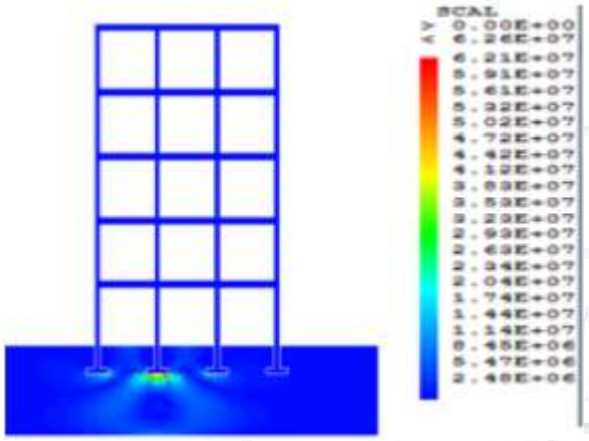

Figure 6(c): Stress values along the XX at 30 s

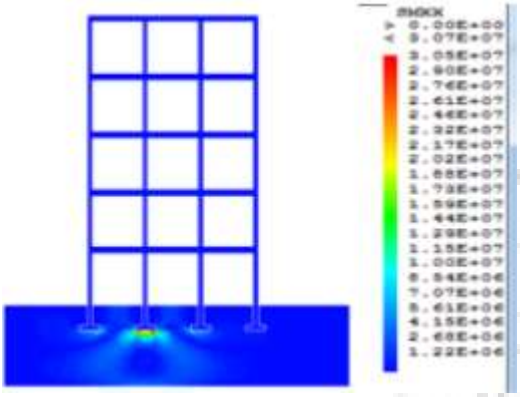

Figure 6(d): Stress values along the axis XX at the time 30 s

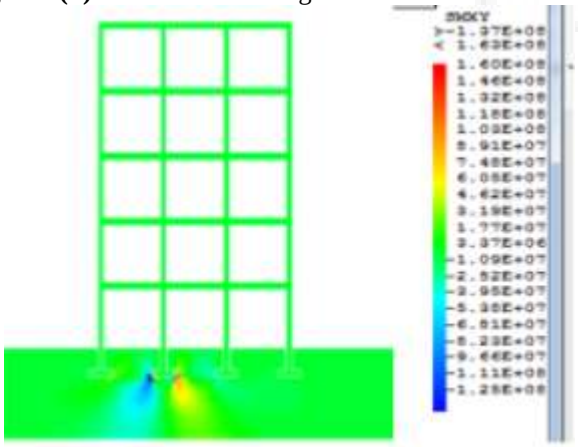

Figure 6(e): The Von Mises's stress along the XY axis at time 30 s

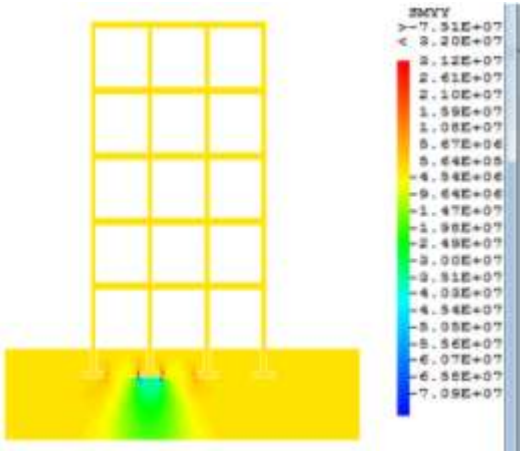

Figure 6(f): The Von Mises's stress along the XY axis at time 30 s

3.3. Deformation diagrams of the framework

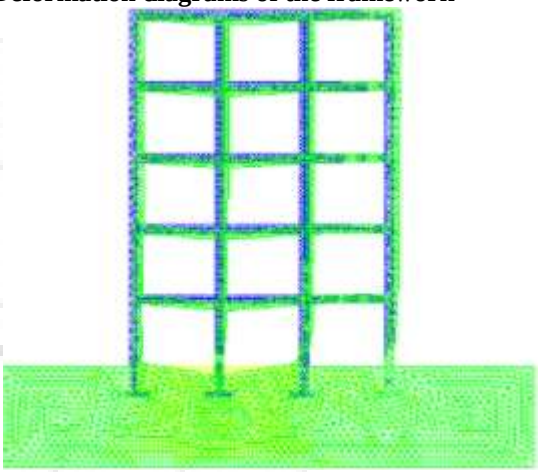

Figure 7 (a): Structure superposition and deformation at the initial time with amplitude

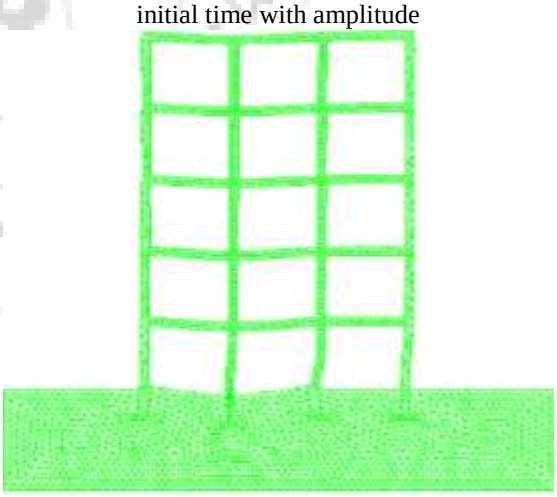

Figure 7 (b): Resultant deformation diagrams, at the initial time whith amplitude

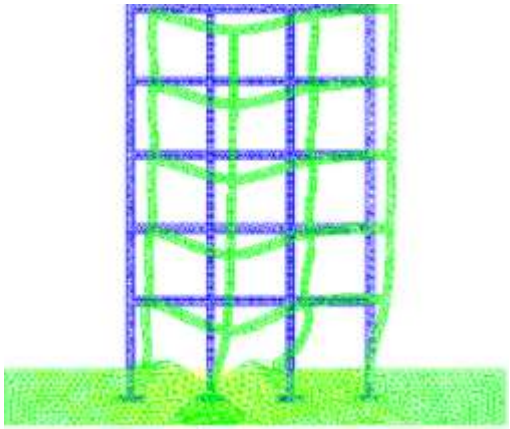

Figure 7 (c): Structure superposition and deformation at the final time with amplitude 93

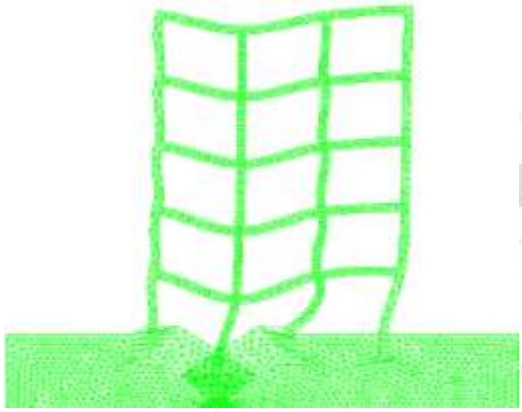

Figure 7 (d): Resultant deformation diagrams, at the final time at amplitude 93

4. Conclusion

In this work, we wanted to describe a progressive collapse from infrastructural origin. With well-chosen materials and soil parameters, the numerical simulation with the Cast3M calculation code permits us to understand the behavior of the sandy clay-structure interface. Our results show that the breaking of the superficial foundations in sandy-clay soil depends mainly on factors such as the loading intensity and the geometry of the foundations. Through the stress-displacement diagrams obtained and the proportional evolution of the stress bubble at the level of the most loaded footing, a set of conclusions emerge: The rupture of the interface results from a succession of phases of deformation of the soil. First a slight settlement which mobilizes the soil in the only descending vertical direction, then because of overloading on a coherent soil (sandy clay), it defines rupture lines which generate a sliding surface more perceptible in a certain direction. The breaking mechanism decreases with increasing depth because the sliding surface is below the influence of the stress bubble. The basic Cam Clay elastoplastic model can help engineers consider structural and constructive arrangements that take into account the geotechnical realities of construction sites. The maximum predictable stress value obtained in the particular case of the sandy clay soil of the city of Douala was $\sigma_{max} = 10$ bars.

References

[1] Nour El Houda Khitas, Etude numérique des fondations superficielles sous charges Combines. Thèse de doctorat : Université Mohamed Khider – Biskra, 2017, pp. 127.
[2] Medjahed A. Approche semi globale 3D pour le calcul des structures en béton armé. Mémoire pour l'obtention du diplôme de Magistère : Université Abou bakr Belkaid en Algérie, 2012, pp. 128.
[3] Allen, T. Influence des dimensions des bâtiments sur la valeur de la période (cas des structures auto-stables). Mémoire de magister : Université de Mouloud Mammeri de Tizi-Ouzou, 2009.
[4] Kaewkulchai G.et Williamson EB, Beam element formulation and solution procedure for dynamic progressive collapse analysis, Computers and structure, vol.82, 2004, pp. 639-651.
[5] Burton, C. Resodt, J. Habert, P. Reiffteck, Calcul des ouvrages géotechniques selon eurocode7 éd Dunod, ISBN 978-2-10-076103-6, 2017, pp. 164.
[6] E. Le Fichoux, (2011) Présentation et Utilisation de Cast3M, Ecole Nationale Supérieure de Techniques Avancées (ENSTA), pp.92.
[7] Xiang Wei Z. Modélisation physique et numérique des interactions sol-structure sous sollicitations dynamiques transverses. Thèse de doctorat : Université de Grenoble, (2011), pp. 177.
[8] Hieng, O.I. Etude des Caractéristiques Géotechniques des Sols du Cameroun, 1ère éd., Yaoundé : Ed CLE, 2013, pp. 147.
[9] P. Fajfar P., Fischinger M. and M. Dolšek, Macro-Models and Simplified Methods for Efficient Structural Analysis in Earthquake Engineering. *Proceedings of the NATO Advanced Research Workshop, Vol.13-17 June 2004, Bled, Slovenia, Vol. 194, NATO Science Series*: Computer and Systems Sciences, 2005, pp. 22-49.
[10] O. C. Zienkiewicz, R. L., Taylor, and J. Z., Zhu. (2005). "Finite Element Method - Its Basis and Fundamentals", 6th edition, (Éd). Elsevier, pp. 802.
[11] Badel B.P. Contributions à la simulation numérique de structures en béton armé. Thèse de Doctorat : Université de Pierre et Marie Curie, Paris VI, 2001, pp. 147.
[12] A. A. Becker. The Boundary Element Method in Engineering. A complete course. Éd. McGraw-Hill, UK, 1992, pp. 69.
[13] Imen SAID. Comportement des interfaces et modélisation des pieux sous charge axiale. Thèse de doctorat : Ecole des Ponts Paris tech, 2006, pp. 275.
[14] Omar Benzaria. Contribution à l'étude du comportement des pieux sous chargements cycliques axiaux. Thèse de doctorat, Université Paris –Est, 2012, pp. 322.
[15] Ligil Mathew, Rinu Mary Varghese, Factors Influencing Sustainability of Infrastructure Projects. *International Journal of Scientific Engineering and Research (IJSER)*, 4(3), 2014. pp. 14-17.
[16] Zasiah Tafheem, Johinul Islam Jihan, Tameem Samdanee, Md. Zahidul Islam & Abu Syed Md. Tarin, Earthquake response analysis of a multistoried RC building under equivalent static and dynamic loading as per Bangladesh national building code 2006. *Malaysian Journal of Civil Engineering*, 28(1), 2016, pp. 108-123.

[17] M. Vincent, J. Bouchut, J.-M. Fleureau, F. Masrouri, E. Oppenheim, J.-V. Heck, N. Ruaux, S. Le Roy, I. Dubus, N. Surdyk, Étude des mécanismes de déclenchement du phénomène de retrait-gonflement des sols argileux et de ses interactions avec le bâti Rapport final BRGM/RP-54862-FR octobre 2003, pp.378.
[18] Hunter, A.H. et Davisson, M.T. (1969). Measurements of pile load transfer. Performance of Deep Foundations, ASTM, STP 444, pp.106-117.
[19] Wolf, J. (1988) soil-structure interaction. Analysis in time domain. Prentice hall international series, Englewood cliffs, New Jersey.